JOURNAL OF VIROLOGY, Sept. 1996, p. 6425–6430 Vol. 70, No. 9
0022-538X/96/$04.00+0

Revertant Analysis of J-K Mutations in the Encephalomyocarditis Virus Internal Ribosomal Entry Site Detects an Altered Leader Protein

MICHAEL A. HOFFMAN[1] AND ANN C. PALMENBERG[2]*

Institute for Molecular Virology and Department of Animal Health & Biomedical Sciences, University of Wisconsin, Madison, Wisconsin 53706[2]; and Department of Molecular Biology, Cleveland Clinic Foundation, Cleveland, Ohio 44195[1]

Received 22 January 1996/Accepted 30 May 1996

The internal ribosomal entry site (IRES) of picornaviruses consists of various sequence and structural elements that collectively impart translational function to the genome. By engineering substitution and deletion mutations into the J-K elements of the encephalomyocarditis virus IRES, translationally defective viruses with small-plaque phenotypes were generated. From these, 60 larger-plaque revertant viruses were isolated and characterized, and their sequences were compared with a structural model of the IRES. The data provide confirming evidence for the existence of helix J3 within stem J but suggest that helix J1 is 3 bp longer than previously estimated. They also suggest that previously modeled stems L and M should be replaced by an alternative structure. One reversion mutation was mapped to the leader protein coding region. This change of leader amino acid 20 from Pro to Ser increased the viral plaque size dramatically but did not alter the cell-free translational activity of the mutated, parental IRES.

Picornavirus RNA translation is initiated by cap-independent, internal binding of ribosomes to an RNA segment within the 5′ untranslated region of the genome (1, 2, 11, 15). Most internal ribosomal entry site (IRES) segments span about 400 nucleotides and contain multiple secondary and tertiary structural elements, which presumably mediate interactions with initiation factors and ribosomal subunits. For picornaviruses, two classes of IRES structures have been proposed according to chemical and enzymatic probing, sequence comparisons, and minimum-free-energy predictions. The group I IRESs of entero- and rhinoviruses share sequences and structural motifs among themselves that are not common to the group II cardio-, aphtho- or hepatovirus IRESs (10). Genetic substitution and revertant analysis have been used effectively to map several functionally important regions within the group I IRESs (4, 5, 17, 18, 21). The group II IRESs have been modeled according to the sequence of encephalomyocarditis virus (EMCV) and phylogenetically related cardioviruses (6, 16), but similar mapping techniques have not been applied to the same extent as with group I IRESs.

Previously, we described six specific substitution mutations and four short deletions that were engineered into one important region of the EMCV IRES, the J-K domain (9). The phenotypes were defined according to in vitro and in vivo translation activity and infectivity of the viral genomes. The mapping highlighted the J and K terminal loops, the J3 helix, and an A-rich bifurcation loop at the J-K junction as particularly critical for translation initiation as directed by this IRES (Fig. 1). During these analyses it was also observed that mutated RNA transcripts varied greatly in their ability to induce plaques on HeLa cells, with phenotypes that ranged from no plaques to plaques of almost wild-type (wt) size. Moreover, with several of these mutations, including G728C (helix J3), U747A (K loop), A772C (A-rich bifurcation loop), and 709Δ7 (J loop), it was noticed that large-plaque viruses occasionally arose against a background of smaller plaques. Although a virus's plaque phenotype may be influenced by several genetic components, it seemed reasonable that among these larger-plaque isolates might be sequences with restored IRES translational activity through direct or second-site reversions.

As now described, 60 larger-plaque isolates which reverted the minute (or nonexistent)-plaque phenotypes of translationally defective mutants were sequenced, reconstructed into viral cDNAs, and then characterized for translational and viability phenotypes. The isolates were plaque purified (two times) before amplification to verify the stability of their phenotypes and their genetic homogeneity. Each was named according to the location of the original mutation (e.g., 709), followed by R, and then a number (e.g., 709R3). If the larger-plaque virus was spontaneously isolated from a smaller-plaque (putative) revertant, an additional letter (e.g., 709R3A) was included, indicating a possible two-step mutational process. The relative plaque sizes (RPS) of all isolates were quantitated on a scale of 0 to 10 relative to that of vM/E, a well-described recombinant-derived strain with wild-type translational and growth characteristics (7–9). Each isolate's IRES (EMCV bases 407 to 873) was then amplified by PCR and sequenced in the region of the original mutation. Candidate sequences for IRES reversions and representative isolates of direct reversions were stabilized in plasmids, resequenced throughout the IRES, and then substituted (along with their parental mutations) back into pEA1.1Eco (9) before additional testing to determine if these changes actually functioned as translational reversions. In the first test, RNA transcripts were quantitated for ability to direct synthesis of the viral L-P1-2A protein in reticulocyte extracts. Increased activity, dependent upon the new mutation, was indication that the alteration(s) was indeed a translational reversion. In a second test, each recombinant IRES in a full-length pM/E context (9) was transfected into cells and the progeny virus was assayed for comparative plaque phenotypes (19) relative to those of the initial isolates.

Revertants of G728C. Mutation G728C destabilized the putative J3 helix by replacement of a C-G base pair with a C-C

* Corresponding author. Mailing address: Dept. of Animal Health and Biomedical Sci., 1655 Linden Dr., Madison, WI 53706. Phone: (608) 262-7519. Fax: (608) 262-7420. Electronic mail address: palmenberg@bioinformatics.bocklabs.wisc.edu.

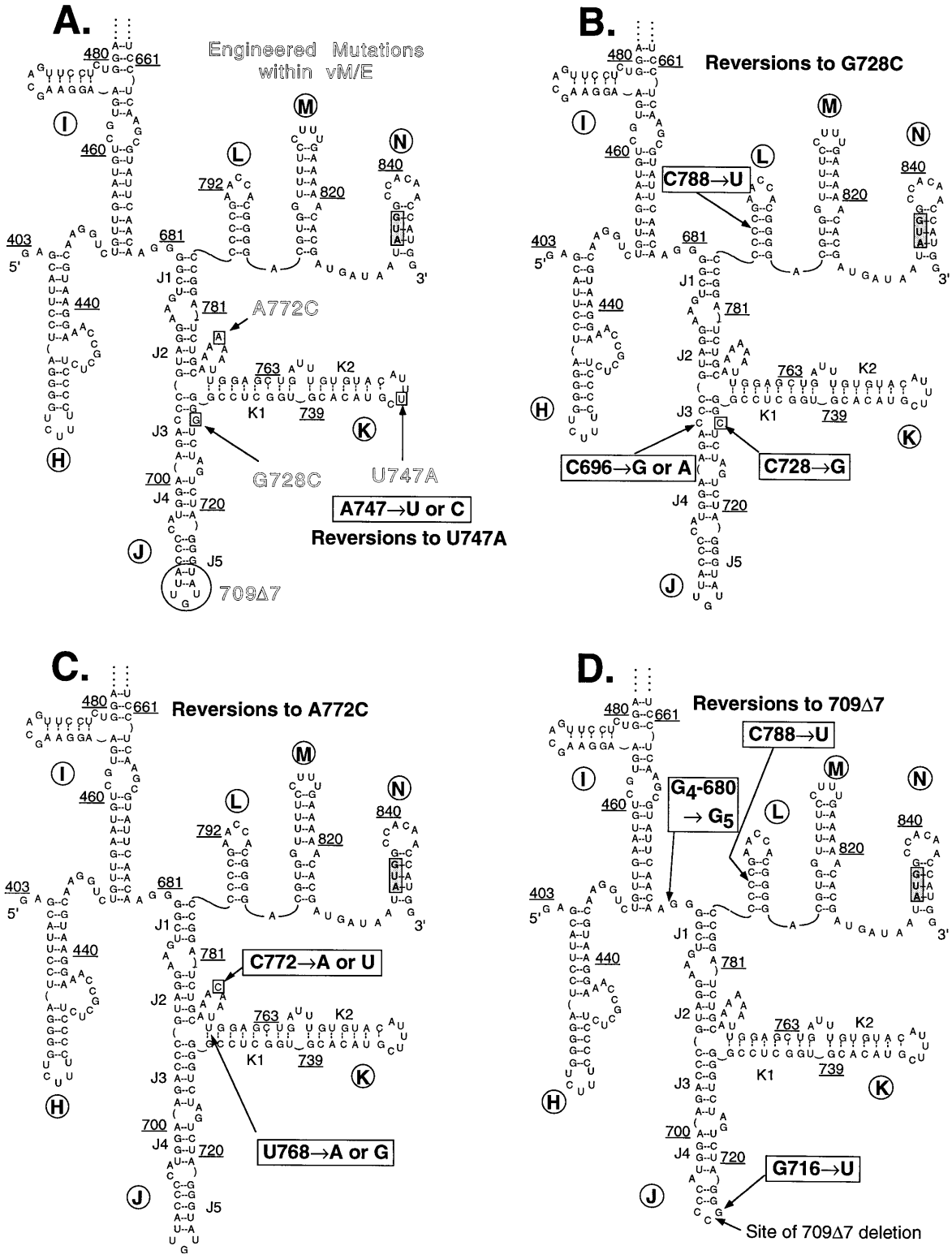

FIG. 1. J-K region of the EMCV IRES. (A) Engineered mutations G728C, U747A, A772C, and 709Δ7 in the J-K IRES segment of vM/E are described elsewhere (9) and named by the mutation (e.g., G-to-C substitution) and location of the altered EMCV-R base (GenBank no. M81861). Sequence numbering is from EMCV-R. (B) Mapped spontaneous IRES reversions to mutation G728C. (C) Mapped spontaneous IRES reversions to mutation A772C. (D) Mapped spontaneous IRES reversions to deletion mutation 709Δ7. Note that this structure is modeled according to the deleted J loop.

TABLE 1. Characteristics of mutant and revertant viruses

Original J-K mutation	Spontaneous larger plaque				cDNA reconstructed	
	Sequence change in IRES	No. of times isolated	Example	RPS[a]	RPS[a]	Relative translation activity[b] [% (no. of tested isolates)]
None	—[c]	—	vM/E (wt)	10	—	100
G728C	—	—	—	0[d]	—	29
	C728G (wt)	1	—	10	—	107 (1)
	Non-IRES	2	—	1	—	31 (2)
	C696G	1	728R4	10	10	90 (1)
	C696A	1	728R6	7	5	51 (1)
	C788U	1	728R1	4	2	56 (1)
U747A	—	—	—	4	—	85
	A747U (wt)	10	—	10	—	ND
	A747C	4	—	9	—	ND
709Δ7	—	—	—	0[d]	—	25
	Non-IRES	6	—	1	—	26 (5)
	C788U	2	709R4A	4	2	55 (2)
	G_4680G_5	1	709R6A	4	2	46 (1)
	G716U	1	709R3A	3	3	58 (1)
A772C	—	—	—	3	—	30
	C772A (wt)	17	—	10	—	98 (2)
	Non-IRES	2	—	5	—	38 (2)
	C772U	2	772R24	5	5	90 (2)
	U768A	2	772R30	10	9	101 (1)
	U768G	6	772R26	10	10	89 (2)
	C891U[e]	1	772R4	7	5	ND
	CCA891AGU[e]	—	P20S	—	5	30 (1)

[a] Plaque size was quantitated on a scale of 1 to 10 relative to that of vM/E (3.2 mm at 30 h posttransfection).
[b] Relative [^{35}S]Met incorporation in reticulocyte extracts. ND, not determined.
[c] —, not applicable.
[d] Plaques only after 50 to 70 h posttransfection with 1 to 2 μg of RNA.
[e] Located in leader protein coding region.

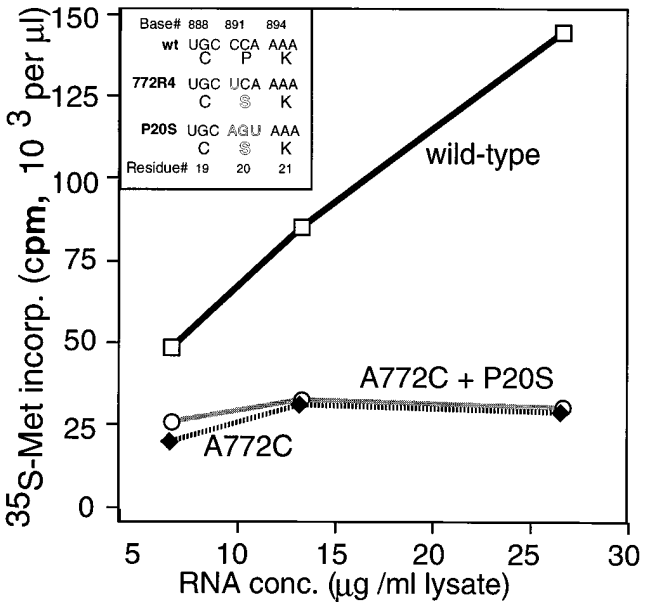

FIG. 2. Non-IRES 772R4 characterization. The *Bss*HII-*Bst*BI fragment from 772R4 that reverted the A772C plaque phenotype was sequenced to find a C891U change in the leader coding sequence. The two-primer method of mutagenesis (Muta-Gene kit; Bio-Rad) was then used to change the same 20th codon from CCA to AGU (P20S) within plasmid pEA1.1Eco (9). The engineered mutation was transferred into pEA1.A772C and pM/E.A772C by exchange of a *Bss*HII-*Bst*BI fragment. Cell-free translations (9, 14) containing [^{35}S]methionine (1 mCi/ml) were programmed with the indicated concentrations of RNA transcripts from vM/E, A772C or A772C containing the engineered P20S sequence. After 60 min at 30°C, the reactions were stopped and quantitated for acid-insoluble radioactivity as described previously (13).

interior loop (Fig. 1B). The substitution had strong, negative effects on IRES-directed translation in vitro and in vivo (9), and mutant-containing transcripts produced plaques only at 50 to 70 h after transfection, and then at a frequency 10^4-fold lower than that of the wild type. The low infectivity suggested that any observed plaques were probably reversions. Viruses from six such plaques were isolated and sequenced (Table 1). One isolate had a direct reversion (C728G), two had restored (C696G) or partially restored (C696A) the base pair disrupted by the G728C mutation, and one virus had a base change (C788U) just outside the J-K domain.

As expected, the sequence with a direct reversion restored full in vitro translational efficiency (107%) and wt plaque size. Since this isolate now contained a normal IRES, it was not characterized further. Of greater interest were the transversion mutations at base 696 which replaced (C696G) or partially replaced (C696A) the original C-G base pair with G-C and A-C pairs, respectively. Of these, C696G had the stronger revertant phenotype. When engineered into a viral context (pEA1.1Eco) along with its parental mutation, this change increased the translational efficiency to 90%, a level indistinguishable from that of vM/E, and also restored the RPS to 10. The engineered A-C pair at the same location (C696A) only partially restored translation (51%) and gave a plaque size (RPS = 5) smaller than that of the original isolate, 728R6. Thus, C696A was a partial translational reversion but alone was insufficient to explain the enhanced plaque phenotype of 728R6. Another unidentified change(s) outside of the IRES must also be present in this virus.

A similar phenotype characterized 728R1, in which sequencing identified a C-to-U change in EMCV base 788. This nucleotide, in stem-loop L, is outside the J-K domain (Fig. 1B). Despite its distance from G728C, engineered C788U gave partial restoration of translation activity (to 56%) and plaque size (to an RPS of 2). Again, however, this change alone (C788U) was insufficient to restore the complete plaque size of the original revertant (RPS = 4). Like C696A, C788U was a translational reversion, but it was only partially responsible for the enhanced plaque phenotype.

The two remaining G728C plaque isolates (RPS = 1) were sequenced throughout their IRESs (EMCV bases 260 to 873), but no changes other than the original mutations were identified. As confirmation, PCR fragments containing these segments were reconstructed into vM/E and tested for cell-free translation. The poor activity (31%) discounted an IRES reversion as the source of these minute plaques, and these isolates were not characterized further.

Revertants of U747A. RNA transcripts containing U747A mutations were only marginally impaired in cell-free reactions. The genotypic defects of these sequences were evident only when translated in vivo or assayed for infectivity (9). HeLa transfection of U747A mutation gave uniformly small plaques (RPS = 4). Of the 14 larger-plaque isolates, 10 were sequenced as direct revertants, restoring wild-type plaque size (RPS = 10) and translational efficiency. The other four revertants had alterations at exactly the same base but replaced a C rather than

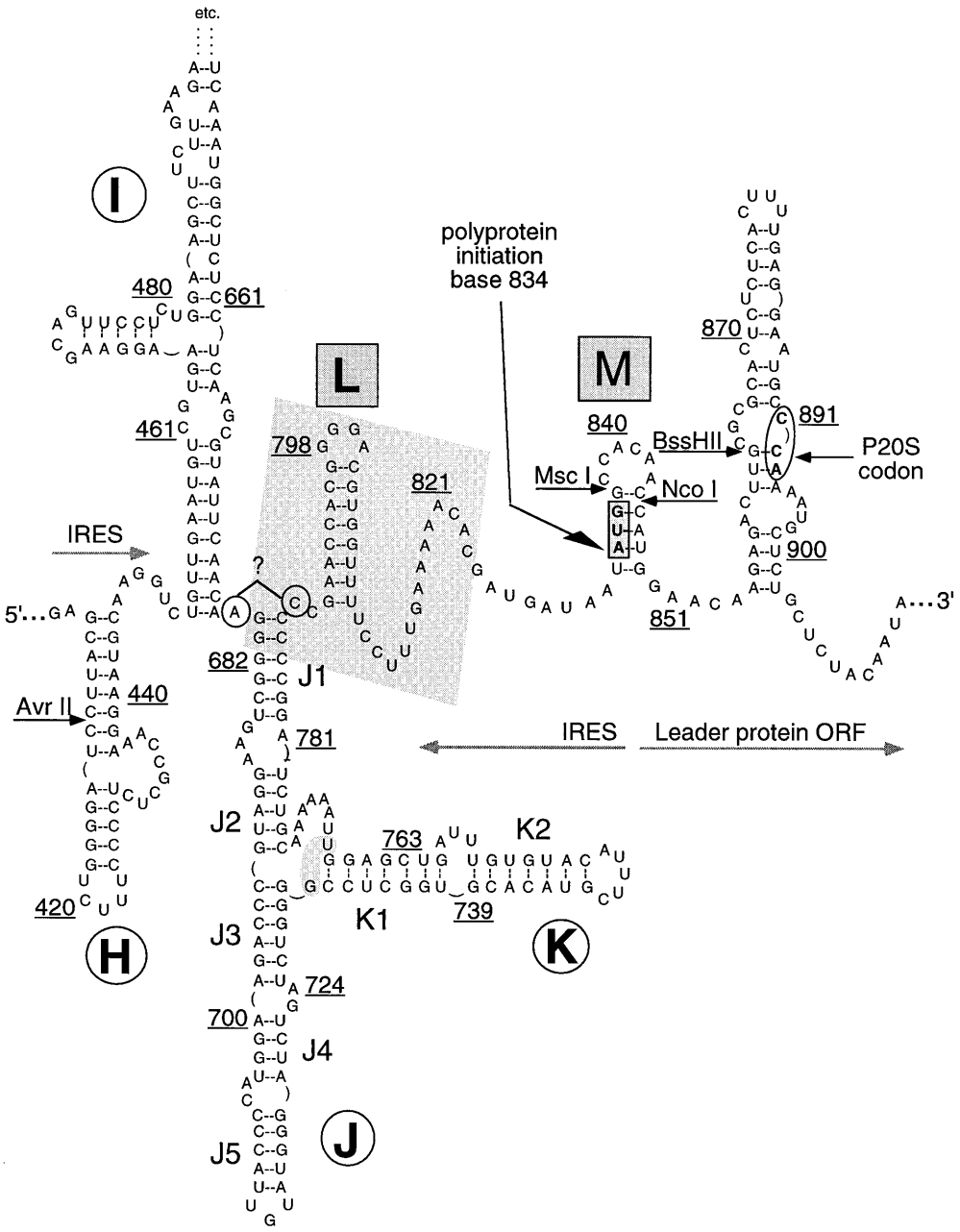

FIG. 3. Revised EMCV J-K model. This model is similar to that previously proposed (6), except within the shaded region, where it is modified according to data presented here and for consistency with alternative published versions (16). The circled bases A680 and C788 mark the location of an additional putative base pair in the G_4680G_5 and C788U reversion sequences. For completeness, a proposed structure near the C891U leader protein reversion sequence is included. ORF, open reading frame.

U. The virtual restoration of wt plaques and the efficient cell-free translation of the parental mutation (U747A, 85%) made finer distinctions among these genotypes (747U, 747C, and 747A) difficult to characterize. Although it had been hoped that reversions at this particular site might point to second-site interactions indicative of a tertiary binding, none of the isolates supported this hypothesis. Each reversion converted the same altered purine (A) into an apparently more acceptable pyrimidine (U or C). Similar pyrimidine-rich substitutions are found in K loops of other naturally occurring cardioviruses (6) and have been suggested to aid eIF-2 recognition by this sequence (20).

Revertants of 709Δ7. Mutant 709Δ7 had a 7-base deletion that included the terminal J loop (Fig. 1D). The sequence was virtually inactive in cellular translational assays, and transfection of full-length RNA containing the 709Δ7 mutation gave only small plaques at 50 to 70 h posttransfection (9). As with G728C, the low specific infectivity suggested that any larger plaques had a high probability of being revertant. Six such viruses were isolated, but after purification and amplification, five of the revertant stocks showed even larger plaques. Five stable, homogeneous revertant stocks were then derived from these larger-plaque viruses.

Sequence analysis showed that six original isolates, with the

smallest plaques (RPS = 1), were unchanged within their IRESs and unable to direct cell-free translation above the level of the parental mutation (26%). Two other isolates were sequenced with the same C788U change in stem-loop L that had been found among the G728C revertants. Similar to the G728C results, this change increased translation efficiency of the 709Δ7 deletion (to 55%), but not to wt levels. Transfer of C788U into the 709Δ7 plasmid increased the plaque size and the infectivity of transcript RNAs but was insufficient to restore the plaque phenotype to that of 709R4A. Overall, the IRES response to this second-site mutation was similar to the G728C context and again clearly indicated that additional changes that affected the plaque size must lie elsewhere in the genome.

Another virus from these stocks, 709R6A, was sequenced with an unusual IRES length alteration. For EMCV and most other cardioviruses, the sequence 5′ of the J1 helix normally terminates with four guanine residues. This particular isolate (RPS = 4) had an additional base within this string (G_4680G_5). The fifth G increased the in vitro translation of the parental J-loop deletion to 46% and was responsible for some but (again) not all increased plaque size and infectivity of 709R6A. Like C788U, incomplete restoration of G_4680G_5 plaque size suggested additional unmapped mutations outside the IRES, although the extra G could surely be tagged as a partial reversion response to the defective translational sequence. The final isolate from this stock (709R3A) had a G-to-U change at base 716, a location immediately 3′ to the original 709Δ7 deletion. When tested from cDNA, the alteration gave a moderate increase in translation activity (58%) and produced plaques equivalent to those of the 709R3A virus from which it was derived.

Revertants of A772C. Transfection of RNAs containing A772C within the J-K oligo(A) bifurcation loop gave minute plaques (RPS = 3) after 30 h of incubation, presumably because of the low efficiency with which this IRES is translated (30%). Still, the specific infectivity of this mutation made larger plaques easy to detect, and 30 isolates were picked, propagated, and sequenced. Of these, 17 were direct reversions to the wt sequence (C772A), and when cloned as cDNAs, the two tested representatives completely restored translational efficiency (98%).

Two other isolates had replaced the C at this location with a U (C772U). The phenotype (RPS = 5; relative translation of 90%) was not as robust as the direct reversions but was still among the most active of tested sequences. Eight other A772C large-plaque isolates (RPS = 10) were mapped to IRES position 768, near the base of the altered bifurcation loop. Two different transversions, U768A and U768G, were sequenced here, and each, when tested in the presence of A772C, was an effective revertant. This location, then, marked a true second-site reversion that seemed to completely compensate for the defective genotype of the original mutation. Since no obvious structural model links base 772 with 768 in optimal or suboptimal folding predictions (6), we propose instead that both sites may be equivalently recognized by a required protein that may bind at or near the bifurcation loop. A defect at one nucleotide might easily be compensated by a commensurately tighter reaction elsewhere within the site. Initiation factor eIF-2 (20), La autoantigen (12), p49 (9), or even the ribosome itself might be candidates for such reactions.

Non-IRES revertants of A772C. IRES-dependent functions were assigned to 49 of the above-described plaque reversions after genetic reconstruction into an otherwise wt genomic background and proof that the altered IRESs had revived translational activities. But 11 larger-plaque isolates had no sequence changes in their IRESs besides the original mutations, and several of the reversion-containing reconstructed IRESs proved insufficient by themselves to fully restore plaque size to that of the original revertant. This partial restoration indicated that additional mutations, outside the IRES, were also present in these viruses. Because of an especially large plaque size, 772R4 (RPS = 7) seemed an ideal candidate to search for such non-IRES reversions.

To achieve this, most of the 772R4 genome was cloned and/or sequenced. PCR techniques amplified nine cDNA segments that collectively covered about 7,500 bases of the RNA, excluding only a short fragment near the 3′ end of capsid precursor P1. Individually, these segments were engineered back into vM/E, containing the parental A772C mutation, and the resultant sequences were tested for plaque morphology. Only one segment of 1,500 bases encompassing the 772R4 leader protein and part of P1 region was reasonably effective in reverting the phenotype (RPS = 5). By analyzing and sequencing progressively smaller fragments, it was found that 772R4 had a C-to-U mutation at base 891 (Fig. 2), resulting in a Pro-to-Ser substitution at the 20th amino acid of the leader protein. This site is only 60 bases 3′ to the viral IRES and 119 bases from the A772C mutation. When engineered back into A772C, C891U was responsible for a substantial increase in viral plaque size (RPS = 5). To establish whether the base itself or the encoded amino acid had caused this effect, the 20th codon of the pM/E leader sequence was changed by mutagenesis from CCA (Pro) to AGU (Ser) and then tested again in the A772C context. The synthetic combination also gave an enhanced plaque phenotype, clearly implicating the altered amino acid as the morphological agent. It was therefore unexpected that P20S (CCA891AGU) was no more translationally active than the parental sequence (Table 1) in an A772C context. Even RNA saturation experiments, which are highly sensitive to subtle differences in translational activation, failed to distinguish A772C activity from that augmented with the plaque-enhancing P20S (Fig. 2). Although this leader amino acid was clearly responsible for the plaque size change in the revertant phenotype, its mechanism did not manifest through an obvious alteration in the transcripts' translational rates, as measured in cell extracts. When tested as a full-length sequence in a vM/E context, P20S gave an RPS of 10, the same as the wt IRES (not shown).

This behavior was puzzling, until a recent report on leader region mutations in the closely related Theiler's murine encephalomyelitis virus provided a potential answer. Within the presumed Theiler's murine encephalomyelitis virus homolog for EMCV leader, H.-H. Chen and colleagues have identified a conserved CHCC (Cys-3–His-5–Cys-10–Cys-13) motif reminiscent of Zn-binding proteins that interact with translating mRNAs. They proposed that the Theiler's murine encephalomyelitis virus leader may serve an autoregulatory translational repression function during cardioviral infection, through a Zn binding mechanism (3). Interestingly, the analogous motif in EMCV (Cys-10–His-11–Cys-19–Cys-22) directly overlaps the P20S location that compensates in plaque size for the A772C translational defect. Should this leader hypothesis prove valid, it might predict that during in vivo infection, a defective leader sequence (e.g., P20S) could putatively compensate for an equally defective IRES (e.g., A772C) through an inability to further repress (depress) viral translation. As we discovered with our engineered combination mutations, such regulatory activities might not be especially evident in reticulocyte extracts. We intend to engineer and test P20S in other vM/E contexts with additional J-K mutations (e.g., G728C) and also scan the leader regions of the remaining non-IRES plaque size revertants for equivalent protein sequence changes.

Revised IRES model. Genetic mapping, particularly through revertant analysis, is commonly used to confirm or refute particular elements of a predicted RNA structural model. We fully expected that among the 60 putative revertants, a large proportion might be at second sites and indicative of putative tertiary interactions. The A772C substitution in the oligo(A) bifurcation loop, for example, is a tempting inverse sequence to the translationally important pyrimidine-rich segment at EMCV bases 807 to 815 (22). But although the revertant data from 30 separate isolates showed a strong pattern of permissible substitutions in and around this bifurcation loop, there was no indication of pairing compensations elsewhere in the IRES. Likewise, the U747A substitution in the loop of the K stem was tagged with 14 same-site changes that gave no indication of exogenous RNA interactions. IRES models for these two loops, then, are consistent with single-stranded regions, and in fact, the bifurcation segment at the J-K junction should probably be extended to include base 768, which the reversions suggest can function as purine or a pyrimidine. The predicted helical nature of the J3 region was also confirmed by these analyses, because the most effective reversions for G728C directly replaced the erroneous base pair with the wt (C-G) or its genetic equivalent (G-C). An improper pair (A-C) was only somewhat restorative. Surprising but equally effective was the mutational creation of an additional J1 base pair (C788U). This same change (C778U), or the alternative insertion of G at the 5′ side of J1, was equally active in reverting the defects imparted by the 709Δ7 deletion. Our previous IRES predictions have modeled four J1 base pairs (6), although others have assigned six pairs, at the expense of L-stem stability (16). The G_4680G_5 and C788U changes are more consistent with a seventh J1 pair, fixed in response to the J3 (G728C) or J5 (709Δ7) disruptions. The previous L loop is not supported by these data, and a revised regional structure is obviously now warranted (Fig. 3). Alterations to the model aside, it is still hard to envision how enhanced stability of J1 could compensate for a J5 defect, 26 bp away, unless protein bridges these segments. The overall structure and surface topography of J-K clearly need to be examined crystallographically before we can understand this function.

This work was supported by National Institutes of Health grant AI-17331 to A.C.P. and NIH training grant GM-07215 to M.A.H.

REFERENCES

1. **Belsham, G. J., and J. K. Brangwyn.** 1990. A region of the 5′ noncoding region of foot-and-mouth disease virus RNA directs efficient internal initiation of protein synthesis within cells: involvement with the role of L protease in translational control. J. Virol. **64:**5389–5395.
2. **Borman, A., and R. J. Jackson.** 1992. Initiation of translation of human rhinovirus RNA: mapping the internal ribosome entry site. Virology **188:** 685–696.
3. **Chen, H.-H., W.-P. Kong, and R. P. Roos.** 1995. The leader peptide of Theiler's murine encephalomyelitis virus is a zinc-binding protein. J. Virol. **69:**8076–8078.
4. **Dildine, S. L., and B. L. Semler.** 1988. The deletion of 41 proximal nucleotides reverts a poliovirus mutant containing a temperature-sensitive lesion in the 5′ noncoding region of genomic RNA. J. Virol. **63:**847–862.
5. **Dildine, S. L., K. R. Stark, A. A. Haller, and B. L. Semler.** 1991. Poliovirus translation initiation: differential effects of directed and selected mutations in the 5′ noncoding region of viral RNAs. Virology **182:**742–752.
6. **Duke, G. M., M. A. Hoffman, and A. C. Palmenberg.** 1992. Sequence and structural elements that contribute to efficient encephalomyocarditis viral RNA translation. J. Virol. **66:**1602–1609.
7. **Duke, G. M., J. E. Osorio, and A. C. Palmenberg.** 1990. Attenuation of mengovirus through genetic engineering of the 5′ noncoding poly(C) tract. Nature (London) **343:**474–476.
8. **Duke, G. M., and A. C. Palmenberg.** 1989. Cloning and synthesis of infectious cardiovirus RNAs containing short, discrete poly(C) tracts. J. Virol. **63:**1822–1826.
9. **Hoffman, M. A., and A. C. Palmenberg.** 1995. Mutational analysis of the J-K stem-loop region of the encephalomyocarditis virus IRES. J. Virol. **69:**4399–4406.
10. **Jackson, R. J., and A. Kaminski.** 1995. Internal initiation of translation in eucaryotes: the picornavirus paradigm and beyond. RNA **1:**985–1000.
11. **Jang, S. K., H. G. Krausslich, M. J. H. Nicklin, G. M. Duke, A. C. Palmenberg, and E. Wimmer.** 1988. A segment of the 5′ nontranslated region of encephalomyocarditis virus RNA directs internal entry of ribosomes during in vitro translation. J. Virol. **62:**2636–2643.
12. **Meerovitch, K., Y. V. Svitkin, H. S. Lee, F. Lejbkowicz, D. J. Kenan, E. K. L. Chan, V. I. Agol, J. D. Keene, and N. Sonenberg.** 1993. La autoantigen enhances and corrects aberrant translation of poliovirus RNA in reticulocyte lysate. J. Virol. **67:**3798–3807.
13. **Palmenberg, A. C.** 1982. In vitro synthesis and assembly of picornaviral capsid intermediate structures. J. Virol. **44:**900–906.
14. **Pelham, H. R. B., and R. J. Jackson.** 1976. An efficient mRNA-dependent translation system from reticulocyte lysates. Eur. J. Biochem. **67:**247–256.
15. **Pelletier, J., and N. Sonenberg.** 1988. Internal initiation of translation of eukaryotic mRNA by a sequence derived from poliovirus RNA. Nature (London) **334:**320–325.
16. **Pilipenko, E. V., V. M. Blinov, T. M. Dmitrieva, and V. I. Agol.** 1989. Conservation of the secondary structure elements of the 5′-untranslated region of cardio- and aphthovirus RNAs. Nucleic Acids Res. **17:**5701–5711.
17. **Pilipenko, E. V., V. M. Blinov, L. I. Romanova, A. N. Sinyakov, S. V. Maslova, and V. I. Agol.** 1989. Conserved structural domains in the 5′-untranslated region of picornaviral genomes: an analysis of the segment controlling translation and neurovirulence. Virology **168:**201–209.
18. **Pilipenko, E. V., A. P. Gmyl, S. V. Maslova, Y. V. Svitkin, A. N. Sinyakov, and V. I. Agol.** 1992. Prokaryotic-like cis elements in the cap-independent internal initiation of translation on picornavirus RNA. Cell **68:**119–132.
19. **Rueckert, R. R., and M. A. Pallansch.** 1981. Preparation and characterization of encephalomyocarditis virus. Methods Enzymol. **78:**315–325.
20. **Scheper, G. C., A. A. Thomas, and H. O. Voorma.** 1991. The 5′ untranslated region of encephalomyocarditis virus contains a sequence for very efficient binding of eukaryotic initiation factor eIF-2/2B. Biochim. Biophys. Acta **1089:**220–226.
21. **Svitkin, Y. V., N. Cammack, P. D. Minor, and J. W. Almond.** 1990. Translation deficiency of the Sabin type 3 poliovirus genome: association with an attenuating mutation C472 to U. Virology **175:**103–109.
22. **Witherell, G. W., A. Gil, and E. Wimmer.** 1993. Interaction of polypyrimidine tract binding protein with the encephalomyocarditis virus mRNA internal ribosomal entry site. Biochemistry **32:**8268–8275.